Conf-950518--6

SAND94-3244C

HIGH RATE ECR ETCHING OF III-V NITRIDE MATERIALS

R. J. Shul, A. J. Howard, and S. P. Kilcoyne
Sandia National Laboratories, Albuquerque, New Mexico 87185-0603

S. J. Pearton, C. R. Abernathy, and C. B. Vartuli
University of Florida, Gainesville, Florida 32611

P. A. Barnes and M. J. Bozack
Auburn University, Auburn, Alabama 36849

The III-V nitride compound semiconductors are attracting considerable attention for blue and ultraviolet light emitting diodes (LEDs) and lasers as well as high temperature electronics due to their wide band gaps and high dielectric constants. The recent progress observed in the growth of these materials has not been matched by progress in processing techniques to fabricate more highly sophisticated devices. Patterning these materials has been especially difficult due to the relatively inert chemical nature of the group-III nitrides. We review dry etch techniques which have been used to pattern these materials including electron cyclotron resonance (ECR), reactive ion etch (RIE), and chemically assisted ion beam etching (CAIBE). ECR etch rates greater than 3800 Å/min for InN, 3500 Å/min for GaN, and 1170 Å/min for AlN are reported. Etch anisotropy, surface morphology, and near-surface stoichiometry will be discussed.

INTRODUCTION

The III-V nitrides continue to generate significant interest in the semiconductor community due to their use in blue and ultraviolet light emitting diodes (LEDs) and lasers as well as high temperature electronics due to their wide band gaps and high dielectric constants.[1-12] Although a great deal of work has been concentrated in this area, the existing processing techniques for these materials are unsuitable for many device applications. The lack of a lattice matched substrate for epitaxial growth, difficulty in implant doping and isolation, poor ohmic and Schottky contacts, and unsuitable patterning techniques have inhibited the fabrication of high performance, reliable photonic and electronic devices more sophisticated than LEDs. Recent advances in the growth of high quality III-V nitrides has resulted in device demonstrations of GaN[13] and double-heterojunction AlGaN/GaN[14] and InGaN/GaN[15] LEDs, and metal semiconducting field effect transistors (MESFETs).[16, 17] The rapid developments in material growth along with advanced device structures including lasers and heterojunction bipolar transistors (HBTs) has increased the need for anisotropic, smooth, high rate etching.

In order to fabricate high density electronic and photonic devices, repeatable, anisotropic etching with reasonably high etch rates are necessary at low dc-bias to minimize plasma-induced damage. Due to the relatively inert chemical nature of the

group-III nitrides, wet chemical etching has been inadequate due to the low etch rates and isotropic profiles. Higher etch rates and more anisotropic profiles have been reported in reactive ion etch (RIE) systems with etch rates approaching 600 Å/min at dc-biases greater than -400 V. The high rates and anisotropic profiles achieved with RIE are attributed to the acceleration of energetic ions from the plasma to the wafer. However, this energetic ion bombardment of the surface can damage the sample and degrade both electrical and optical device performance. Attempts to minimize such damage by reducing the ion energy or increasing the chemical activity in the plasma often results in a loss of etch rate or anisotropy which significantly limits critical dimensions and reduces the utility of the process for device applications requiring vertical etch profiles. It is therefore necessary to develop plasma etch processes which couple anisotropy for critical dimension and sidewall profile control and high etch rates with low-damage for optimum device performance.

A great deal of interest has been generated in low-damage etch processes based on high-density-plasmas, such as electron cyclotron resonance (ECR) plasmas, inductively coupled plasmas (ICP), or magnetrons. Due to the magnetic confinement of electrons in the microwave ECR source, high density plasmas are formed at low pressures with low plasma potentials and ion energies. Therefore, less damage than that produced by RIE plasmas has been observed during ECR etching of III-V materials.[18-22] Ion densities in excess of 5×10^{11} cm^{-3} are achieved thereby increasing the potential etch rate due to higher ion flux. Highly anisotropic etching can be achieved in the ECR by superimposing an rf-bias (13.56 MHz) on the sample and employing low pressure conditions to minimize ion scattering which contributes to lateral etching. With rf-biasing, energetic ions are accelerated from the plasma to the sample with potential for kinetic damage to the surface; however, sidewall damage may be low due to the directional nature of the beam, the chemical component of the etch, and the low process pressure.

ECR-generated Cl_2 plasmas have been very successful in etching GaAs and AlGaAs due to the high volatility of the group-III and group-V chlorides. With the addition of H_2 to this plasma chemistry, GaN and AlN etching have been reported where the Ga and Al are removed as group-III chlorides and the N as NH_X.[23] Etching In-containing compounds at room temperature in a Cl_2 based plasma is often accompanied by roughened surfaces due to the low volatility of the In-chlorides and the preferential loss of the group-V species. A low temperature CH_4/H_2 plasma chemistry has been used for smooth, anisotropic etching of InN compounds with low etch rates.[24] This etch chemistry requires strict control of the gas ratio to minimize polymer deposition. High temperature etching of In-containing species has been quite successful using Cl_2 based chemistries due to the higher volatilities of In-chlorides at temperatures above 150°C.[25] In this paper we will report recent progress in ECR etching of binary and ternary III-V nitrides.

EXPERIMENTAL

The binary and ternary films etched by ECR in this study were grown using metal organic molecular beam epitaxy (MO-MBE) on either GaAs or Al_2O_3 substrates in an

Intevac Gen II system described previously.[26] The group-III sources were triethylgallium, trimethylindium, or trimethylamine alane, respectively, and the atomic nitrogen was derived from an ECR Wavemat source operating at 200 W forward power. The layers are single crystal with a high density of stacking faults and microtwins. The GaN and AlN are resistive as-grown, while the InN is highly auto-doped n-type (> 10^{20} cm^{-3}) due to the presence of native defects.

The ECR plasma reactor used in this study was a load-locked Plasma-Therm SLR 770 etch system with an ECR source operating at 2.45 GHz. Energetic ion bombardment was provided by superimposing an rf-bias (13.56 MHz) on the sample. Samples were mounted using vacuum grease on an anodized Al carrier that was clamped to the cathode and heated with He gas. Etch gases were introduced through an annular ring into the chamber just below the quartz window. To minimize field divergence and to optimize plasma uniformity and ion density across the chamber, an external secondary collimating magnet was located on the same plane as the sample and a series of external permanent rare-earth magnets were located between the microwave cavity and the sample. ECR etch parameters used in this study were: 10 sccm of Cl_2, 15 sccm of H_2, 10 sccm of Ar, 0 or 3 sccm of CH_4, 30 to 170°C electrode temperature, 1 to 10 mTorr total pressure, 125 to 850 W of applied microwave power, and 0 to 275 W rf-power with corresponding dc-biases of -15 to -250 ± 10 V. Due to the high etch temperatures, a Si_3N_4 etch mask was employed.

Etch rates were calculated from the depth of etched features measured with a Dektak stylus profilometer after the Si_3N_4 masking material was removed in a SF_6/O_2 RIE plasma. Samples etched in the ECR were approximately 1 cm^2 and depth measurements were taken at a minimum of three positions. Error bars for the etch rates represent the standard deviation across the sample. Several plasma conditions were repeated with better than ±10% sample-to-sample variation. Surface morphology, anisotropy, and sidewall undercutting were evaluated with a scanning electron microscope (SEM). RMS surface roughness was quantified using a Digital Instruments Dimension 3000 atomic force microscope (AFM) system operating in tapping mode with Si tips. Auger Electron Spectroscopy (AES) was used to investigate the near-surface stoichiometry before and after etching of the GaN films.

III-V NITRIDE ETCHING

The III-V nitride materials are chemically inert and resist etching in common compound semiconductor material wet chemical etchants at room temperature. Very slow etching of GaN has been reported in hot alkalis or electrolitically in NaOH.[27, 28] AlN etching has been reported in several different solutions including H_3PO_4, HF/H_2O, HNO_3/HF, and dilute NaOH at relatively low rates.[29-35] Recently, we have reported temperature dependent etching of AlN in AZ400K photoresist developer at controlled rates.[36] The etch is highly selective to GaN and InN and isotropic.

The first RIE etching of GaN were reported by Adesida and co-workers in $SiCl_4$, $SiCl_4$/Ar, and $SiCl_4$/SiF_4 plasmas.[37] Etch rates increased monotonically with increasing dc-bias exceeding 500 Å/min at -400 V. Etch rate was independent of pressure (20 to 80 mTorr) and plasma chemistry. Etches were smooth with an overcut profile due to the physical component of the etch mechanism. Lin *et. al.* have reported similar results in BCl_3 and $SiCl_4$ plasmas with increasing GaN etch rates as the rf-power was increased.[38] Etch rates as high as 1050 Å/min were reported with the BCl3 plasma, whereas the etch rates in $SiCl_4$ were slower. Etch rates decreased with increasing pressure presumably due to lower dc-bias. Ping *et. al.* have reported GaN etch rates in HBr, HBr/Ar, and HBr/H_2 exceeding 600 Å/min at -400 V dc-bias.[39] Once again, the etch rate increased with increasing dc-bias. The addition of either Ar or H_2 to the Br plasma lowered the etch rate under all plasma conditions studied. The best etch rates were obtained at high dc-biases in all studies indicating the highly physical nature of the etch requiring conditions which could induce significant plasma damage to the samples.

The first ECR etching of InN, AlN, and GaN were reported by Pearton and co-workers using low pressure CH_4/H_2/Ar, BCl_3/Ar, Cl_2, and Cl_2/H_2 plasmas.[40] The etch rates for all three materials increased with increasing dc-bias. Etch rates increased significantly and the surfaces became smoother as H_2 was added to the Cl_2 plasma implying more efficient removal of the N etch product. The etch rates were in the range of 100 to 400 Å/min at 1 mTorr and -150 V dc-bias for Cl_2/H_2 while higher biases were necessary for the CH_4/H_2/Ar plasma. Etch rates were further enhanced by increasing the microwave power from 200 to 1000 W.[41] Etch rates of 1100 Å/min for AlN and 700 Å/min for GaN at -150 V in a Cl_2/H_2 plasma and 350 Å/min for InN in a CH_4/H_2/Ar plasma at -250 V were reported. The etched surfaces remained stoichiometric following exposure to the plasma. Pearton *et. al.* also studied etch rates for $In_xGa_{1-x}N$ and $In_xAl_{1-x}N$ alloys in CH_4/H_2, Cl_2/H_2, and Cl_2/SF_6 ECR generated plasmas.[42] For high mole fraction In, CH_4/H_2/Ar plasmas etched faster while at lower In concentration etch rates were faster in the Cl_2/H_2 plasma. The substitution of SF_6 for H_2 in the Cl_2 plasma resulted in higher etch rates while maintaining smooth morphologies. This implies that the removal of N may occur as either NH_x or NF_x.

In addition to ECR high density plasmas, GaN etching has been reported by McLane *et. al.* in a magnetron RIE system[43] and by Adesida *et. al.* using chemically assisted ion beam etching (CAIBE).[44] Etch rates of 3500 Å/min have been achieved in the magnetron RIE using BCl_3 plasmas at dc-biases less than -100 V and 5 mTorr pressure. Auger analysis showed a lower Ga:N ratio for samples exposed to the plasma up to a depth of approximately 100 Å. Using CAIBE, GaN etch rates as high as 2100 Å/min were reported at 500 eV Ar ion beam directed onto the sample in a Cl_2 ambient. Etch rates increased with beam current, Cl_2 flow rate, and substrate temperature. Anisotropic profiles with smooth etch morphologies were observed.

We have reported ECR etching of GaN, InN, and AlN as a function of substrate temperatures ranging from 30 to 170°C.[45] Etch rates for GaN and AlN are shown in

Figure 1 as a function of temperature. The GaN samples were etched in $Cl_2/H_2/CH_4/Ar$ and $Cl_2/H_2/Ar$ plasmas while the AlN samples were etched only in $Cl_2/H_2/CH_4/Ar$ plasmas due to limited sample availability. The etch rates for AlN samples show a monotonic decrease of approximately a factor of two as the temperature is increased from 30 to 170°C. The maximum etch rate is 960 Å/min at 30°C. The GaN etch rate in the $Cl_2/H_2/CH_4/Ar$ plasma is relatively constant up to approximately 125°C and then increases by 14% (to a maximum of 2340 Å/min) as the temperature is increased to 170°C. When CH_4 is removed from the plasma chemistry, the rates decrease by approximately 20 to 40% and show a monotonic increase as the temperature is increased. The increase in the GaN etch rate at high temperature may be attributed to either an increase in the volatility of one of the etch products or a transition in the dominant reaction mechanism.

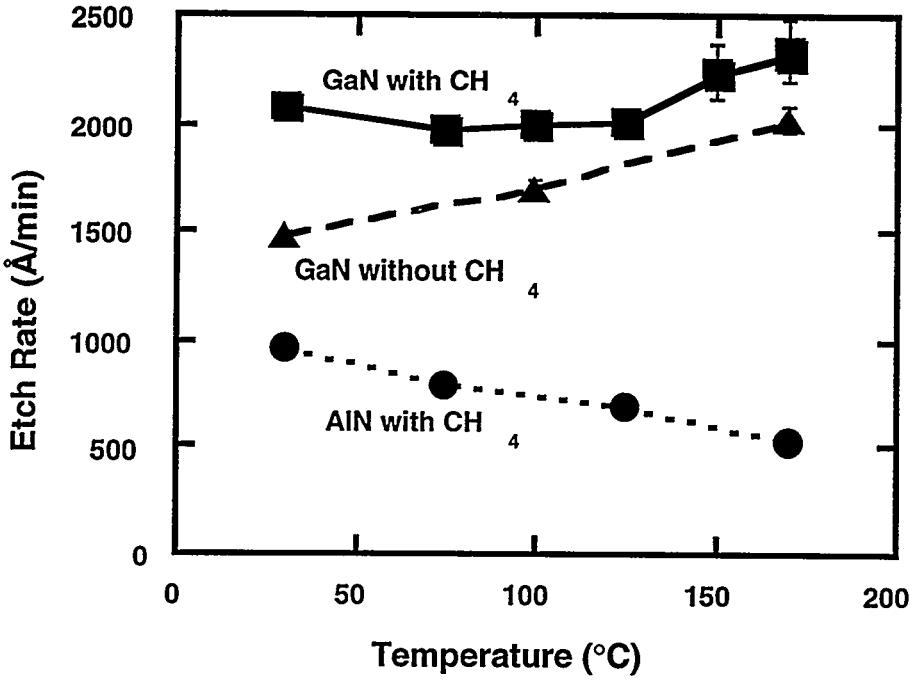

Figure 1. Etch rates of GaN and AlN as a function of temperature for ECR generated $Cl_2/H_2/CH_4/Ar$ or $Cl_2/H_2/Ar$ plasmas.

In Figure 2 the InN etch rates are shown as a function of temperature for the same plasma chemistries. The InN etch rate decreases by more than 60% as the temperature is increased to 150°C for the $Cl_2/H_2/CH_4/Ar$ plasma chemistry, however the etch rate increases rapidly above 150°C to a maximum of 2300 Å/min at 170°C. A similar trend is observed in the $Cl_2/H_2/Ar$ plasma chemistry at etch rates 20 to 50 % lower than those obtained with CH_4 in the plasma. The higher GaN and InN etch rates observed with the presence of CH_4 in the plasma, regardless of the temperature, may be attributed to the additional formation of the group III-methyl etch product which appears to be more volatile than the group III-chlorides below ~150°C or an etch mechanism which is enhanced by the

CH_4. The initial InN etch rate decrease observed in the $Cl_2/H_2/CH_4/Ar$ plasma chemistry may be due to competitive reactions between Cl_2 and CH_4 with InN to form either $InCl_x$ or $In(CH_x)_y$. As the temperature is increased above 150°C, either the volatility of one of the etch products increases or the reaction kinetics become dominated by one of the surface reaction mechanisms. The general observation of higher etch rates for InN at 170°C in both plasma chemistries agrees with higher volatility of the $InCl_x$ etch product observed in Cl_2 etching of InP.[24] For InN surfaces etched at 170°C, the etch without CH_4 resulted in a much rougher surface than the etch with CH_4. We note that the InN etch rates obtained here represent the fastest obtained for this material and suggests that the $Cl_2/H_2/CH_4/Ar$ plasma might be needed to obtain high etch rates in heterostructures containing the In-based ternaries InGaN and InAlN.

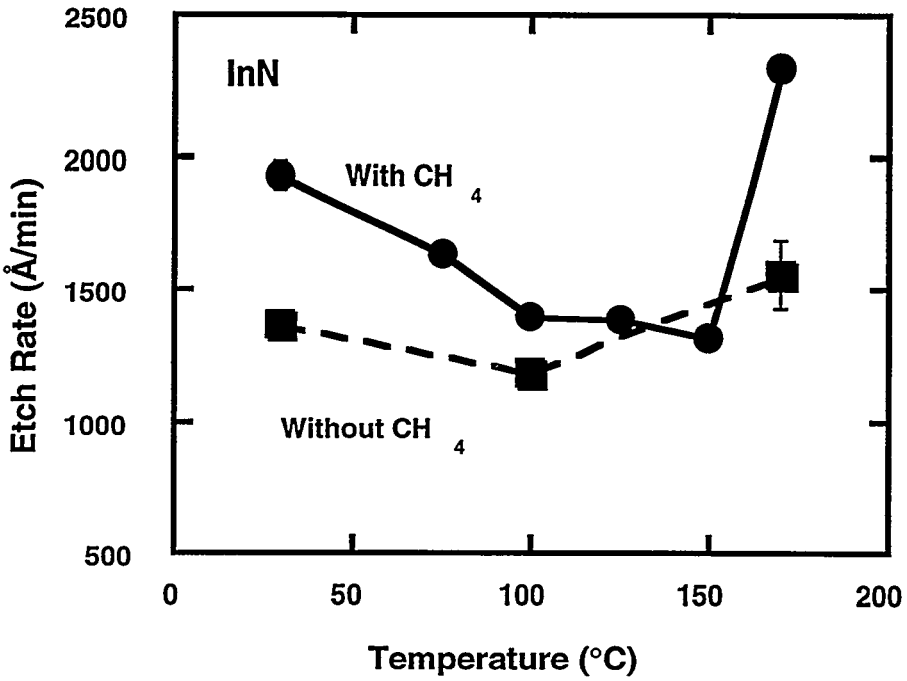

Figure 2. Etch rates of InN as a function of temperature for ECR generated $Cl_2/H_2/CH_4/Ar$ or $Cl_2/H_2/Ar$ plasmas.

High etch rates for III-V nitride binary materials have been reported as a function of pressure, rf-power, and microwave power in an ECR.[46] Etch rates for GaN, InN, and AlN are shown as a function of pressure in Figure 3 for a $Cl_2/H_2/CH_4/Ar$ plasma at 170°C and 850 W of applied microwave power. During these runs the rf-power is held constant at 150 W which results in an increase in dc-bias as the pressure is increased. Higher dc-biases are attributed to increased collisional recombination which decreases the plasma density at higher pressures.[47] Etch rates increase for GaN and AlN as the pressure is increased from 1 to 2 mTorr suggesting a reactant limited regime at 1 mTorr. However, the InN etch rate remains relatively constant at 1 and 2 mTorr possibly due to differences in the etch mechanism or the volatility of the group-III chloride etch products. As the pressure is increased above 2 mTorr, the etch rates for all three materials drop due either to

lower ion densities or to increased polymer deposition at higher pressures.[25, 48] A decrease in etch rates with increasing pressure and dc-biases implies that group-III nitride etching is strongly dependent on plasma density.

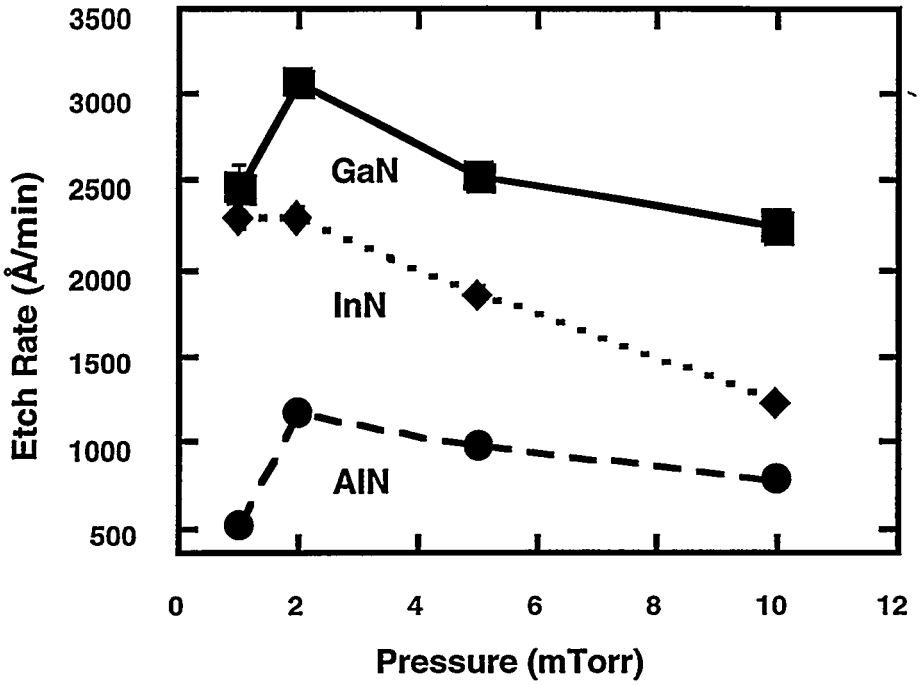

Figure 3. Etch rates of GaN, InN and AlN as a function of pressure for an ECR generated $Cl_2/H_2/CH_4/Ar$ plasma.

In Figure 4, etch rates are plotted as a function of rf-power for GaN, InN, and AlN. Similar to the data discussed previously for RIE, ECR, and CAIBE etching, as the rf-power is increased the etch rates increase monotonically for GaN and InN due to the higher ion energies. Without rf-biasing, the dc-bias is approximately -10 to -15 V and the GaN and InN samples do not etch during a 2 minute exposure; however, when 65 W of rf-power is applied (~ -75 V dc-bias) the GaN etches at a rate of 810 Å/min and the InN etches at 360 Å/min. This suggests either that the etch products are not desorbed efficiently at low ion energy or that a thin surface oxide is present which must be sputtered away before chemical etching can occur. High etch rates for GaN (2850 Å/min) and InN (3840 Å/min) have been achieved at 275 W rf-power. The etch rate for AlN is essentially constant, 240 Å/min, at 0 and 65 W rf-power, increases to 1245 Å/min at 225 W, and then decreases to 635 Å/min at 275 W. AlN etching observed at 0 rf-power implies that either the surface oxide is removed at low dc-bias or the desorption of etch products is more efficient than that for GaN and InN. The decrease in AlN etch rate at 275 W may be related to sputter desorption of active species before they have time to react at the semiconductor surface. In Figure 5, we observe a general increase in etch rate as the microwave power and therefore the ion density is increased. This trend agrees with decreasing etch rates which were observed at higher pressures and lower ion densities. The etch rate for GaN and AlN increases moderately (less than a factor of 2) as the microwave

power is increased from 125 to 850 W, whereas the InN etch rate increases monotonically from 1040 to 3670 Å/min.

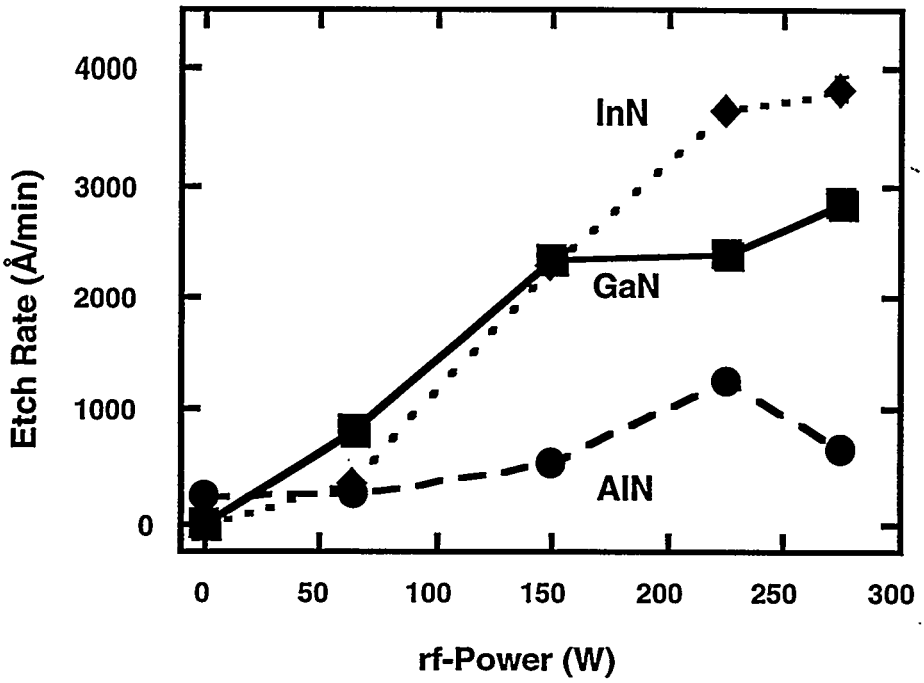

Figure 4. Etch rates of GaN, InN and AlN as a function of rf-power for an ECR generated $Cl_2/H_2/CH_4/Ar$ plasma.

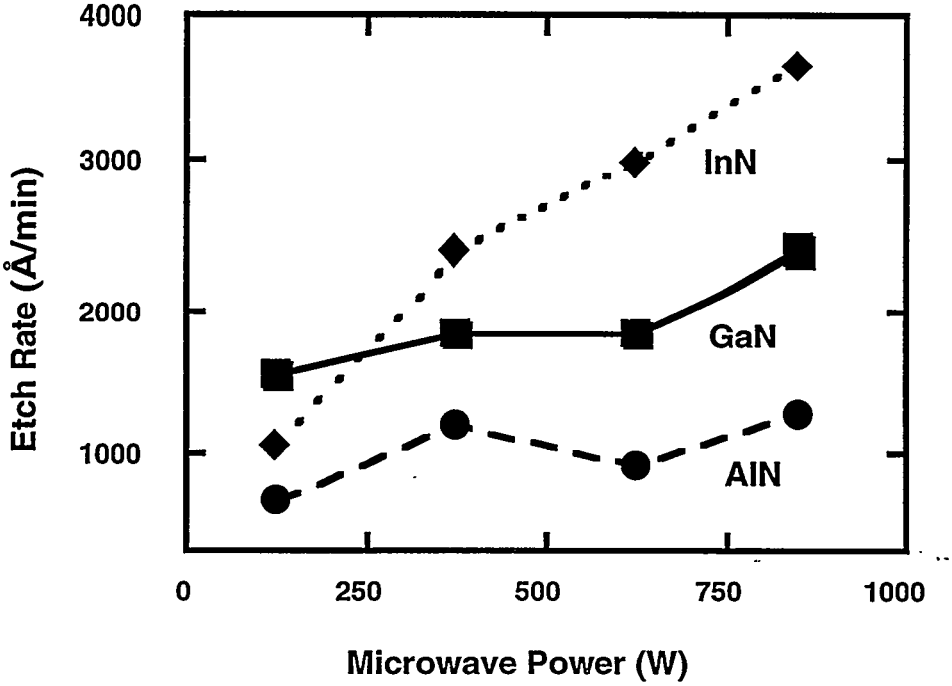

Figure 5. Etch rates of GaN, InN and AlN as a function of microwave power for an ECR generated $Cl_2/H_2/CH_4/Ar$ plasma.

We have also studied temperature dependent (30 to 170°C) etching for the $In_xGa_{1-x}N$ alloys. In Figure 6, etch rates are shown for increasing In concentration, where x equals 0, 0.36, 0.47, 0.65, and 1.0, at 850 W microwave power, 150 W rf-power, and 1 mTorr pressure in a $Cl_2/H_2/CH_4/Ar$ ECR plasma. The etch rates for the InGaN films show a slight decrease with increasing In concentration regardless of the temperature. This may be attributed to the lower volatility of the In etch products as compared to the Ga-chloride. Within experimental error, the etch rates show only a slight temperature dependence where the highest etch rates occur at 170°C.

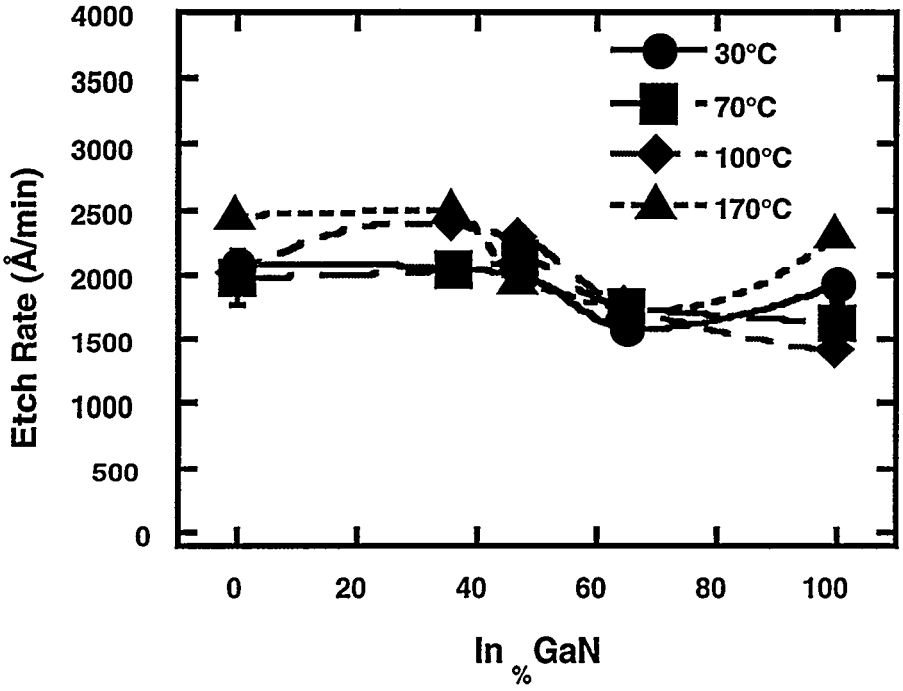

Figure 6. Etch rates for $In_xGa_{1-x}N$ as a function of temperature for an ECR generated $Cl_2/H_2/CH_4/Ar$ plasma.

ETCH PROFILE

Figure 7 shows SEM micrographs of GaN and InN samples etched in $Cl_2/H_2/CH_4/Ar$, at 170°C and 150 W rf-power. The GaN etch is approximately 5800 Å deep and is anisotropic with reasonably smooth sidewalls and surfaces. The high anisotropy of the etch may be attributed to the possible formation of a sidewall polymer involving the methane, as previously reported by Constantine *et al.* with this plasma chemistry.[25, 48] A trench is observed at the base of the GaN feature which may occur due to the Si_3N_4 mask-edge erosion. The InN etch is somewhat rough with a sloped sidewall possibly also due to erosion of the mask-edge. The InN is etched approximately 1.12 μm deep, which is approximately 1000 Å into the GaAs substrate. The surface roughness

therefore most likely is due to etching GaAs under high temperature Cl_2 plasma conditions or to preferential etching of the InN. Using identical etch conditions with 275 W of rf-power, the GaN and InN SEM micrographs in Figure 8 show much rougher surfaces. The corresponding etch rates are significantly higher with improved anisotropy due to the increased ion bombardment energy. However, high ion bombardment energy also contributes to the increased surface roughness, probably due to micro-masking from redeposition of sputtered materials or preferential etching of the group-III nitride film. These etch profiles compare favorably with those obtained in earlier ECR and CAIBE studies and tend to be more anisotropic than those etched in a RIE.

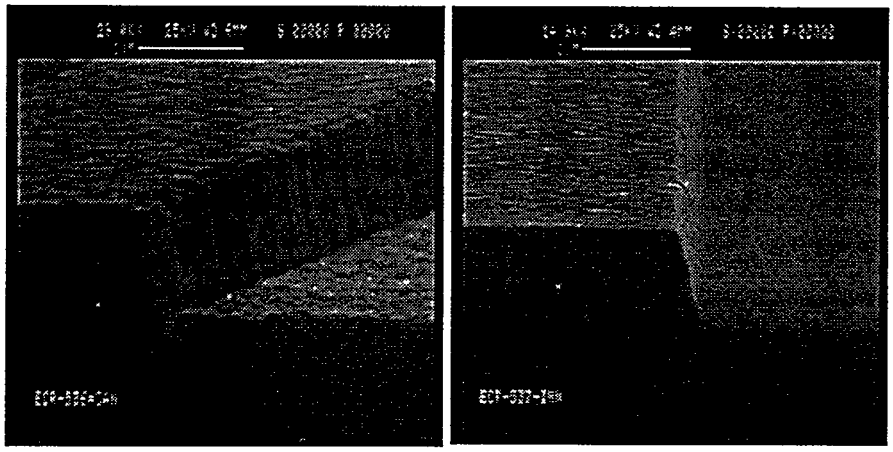

(a) (b)

Figure 7. SEM micrographs of (a) GaN and (b) InN etched at 150 W rf-power in an ECR generated $Cl_2/H_2/CH_4/Ar$ plasma.

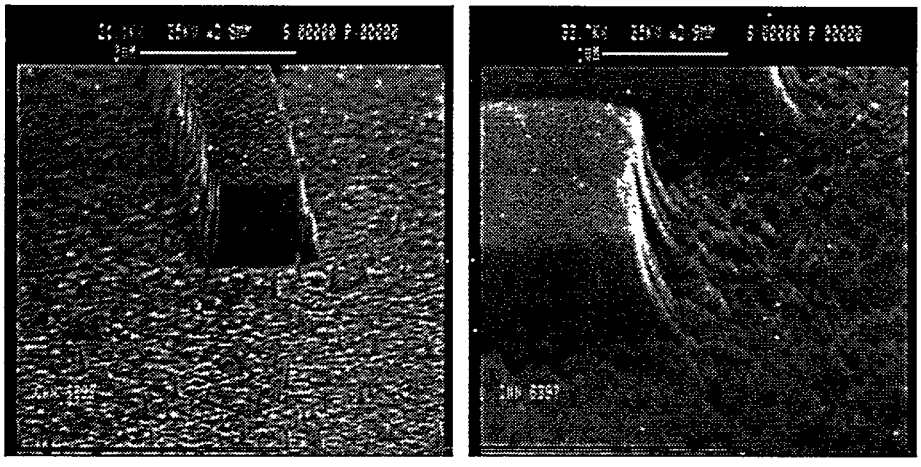

(a) (b)

Figure 8. SEM micrographs of (a) GaN and (b) InN etched at 275 W rf-power in an ECR generated $Cl_2/H_2/CH_4/Ar$ plasma.

SURFACE MORPHOLOGY

The surface morphology as a function of plasma etch conditions is evaluated using AFM. The RMS roughness for GaN and InN as-grown is 3.21 ± 0.56 and 8.35 ± 0.50 nm, respectively. In Figure 9, the RMS roughness is shown as a function of pressure. As the pressure is increased and the rf-power remains constant, we observe an increase in the dc-bias due to lower plasma density. The GaN RMS roughness remains virtually unchanged at approximately 4 nm over the pressure range studied, very similar to the as-grown RMS roughness. The InN RMS roughness, which is consistently higher than that for GaN, increases monotonically as the pressure is increased. At 1, 5, and 10 mTorr, the GaN etch rate remains relatively constant as does the RMS roughness. However, for InN, the etch rate decreases monotonically while the RMS roughness increases implying preferential etching of the InN or inefficient sputter desorption of the etch products due to lower ion densities.

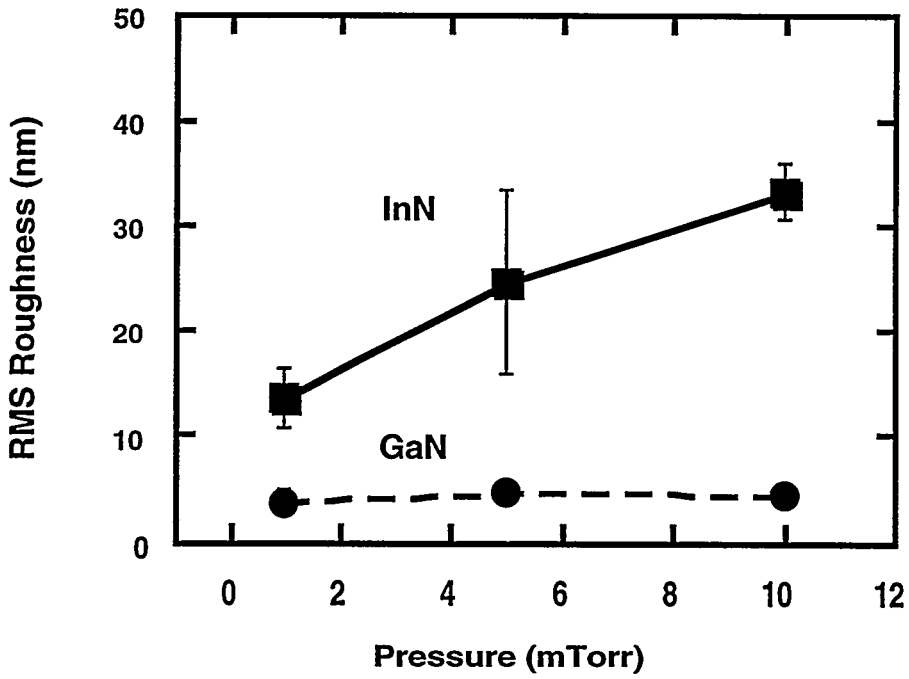

Figure 9. RMS roughness for GaN and InN as a function of pressure in an ECR generated $Cl_2/H_2/CH_4/Ar$ plasma. The as-grown RMS roughness for GaN is 3.21 ± 0.56 nm and for InN is 8.35 ± 0.50 nm.

In Figure 10, the GaN RMS roughness remains relatively constant as the rf-power is increased from 0 to 150 W, however as the rf-power is increased further to 275 W the

RMS increases to approximately 85 nm. The data suggests that at high rf-power, greater *than 200 W, and high etch rates*, preferential sputtering or micro-masking occurs which roughens the surface. At 275 W rf-power, the SEM micrograph shown in Figure 8a shows a lower density of roughness or "spikes" near the etched feature than the AFM image which was scanned in an open 10 x 10 μm area. This may be attributed to a proximity effect of the etch where redeposition is worse in the open areas. The "spikes" near the etched feature were approximately 2000 to 3000 Å tall. The RMS roughness for InN is greatest at 65 W rf-power implying that the ion-bombardment energy is critical to balance the chemical and sputtering effect of this plasma chemistry to maintain smooth surfaces and reasonable etch rates. This trend does not agree with the etch rate data which increases monotonically with rf-power. Further studies are in progress to evaluate preferential etching of the group-III nitrides and to optimize the plasma chemistry. The GaN and InN RMS roughness show identical trends as a function of microwave power as can be seen in Figure 11. Both samples show the roughest surface morphologies at 625 W microwave power and the smoothest surfaces at 850 W where the ion density is highest. The rf-power was held constant at 225 W during these runs.

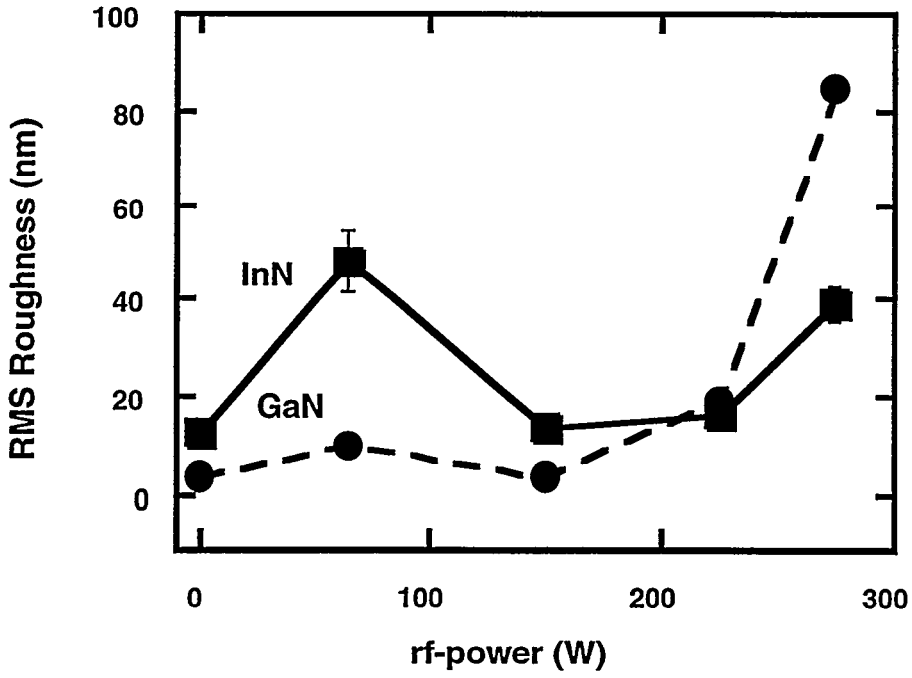

Figure 10. RMS roughness for GaN and InN as a function of rf-power in an ECR generated $Cl_2/H_2/CH_4/Ar$ plasma. The as-grown RMS roughness for GaN is 3.21 ± 0.56 nm and for InN is 8.35 ± 0.50 nm.

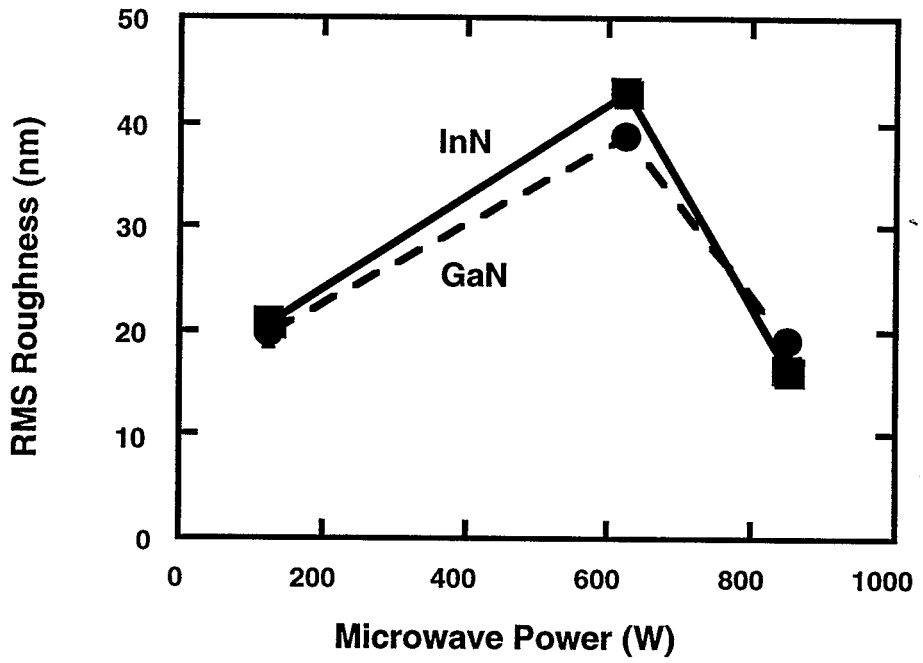

Figure 11. RMS roughness for GaN and InN as a function of microwave power in an ECR generated $Cl_2/H_2/CH_4/Ar$ plasma. The as-grown RMS roughness for GaN is 3.21 ± 0.56 nm and for InN is 8.35 ± 0.50 nm.

FILM STOICHIOMETRY

Prior to exposure of the GaN to the plasma, the Auger spectrum shows a Ga:N ratio of 1.5 with normal amounts of adventitious carbon and native oxide on the GaN surface. Following exposure to the plasma we observe a general tendency for the Ga:N ratio to increase with rf-power and microwave power with some residual atomic Cl from the plasma. The Ga:N ratio increases from 1.8 to 2.3 as the rf-power is increased from 65 to 275 W at a microwave power of 850 W. The ratio also increases from 2.3 to 3.5 as the microwave power increases from 125 to 625 W at a rf-power of 225 W. Within experimental error these trends imply that the GaN film is being depleted of N perhaps due to preferential etching or sputtering of the lighter N-atoms due to higher ion-bombardment energy and higher ion density. The Ga:N ratio does not change as a function of temperature.

CONCLUSIONS

In summary, ECR etching of III-V nitrides are reported as a function of temperature, pressure, microwave power, and rf-power in a $Cl_2/H_2/CH_4/Ar$ plasma. Etch rates of 2850 Å/min for GaN and 3840 Å/min for InN have been obtained at 1 mTorr, 850 W of applied microwave power, and 275 W rf-power. The maximum AlN etch rate

obtained in this study is 1245 Å/min at 1 mTorr, 850 W of applied microwave power, and 225 W rf-power. These are the highest etch rates reported for these materials. The data suggests that ion bombardment energies greater than approximately -15 V are necessary to initiate etching of GaN and InN and that the etch mechanism for group-III nitrides is heavily dependent upon plasma density. As the temperature is increased, the initial decrease in InN and GaN etch rates for the $Cl_2/H_2/CH_4/Ar$ plasma suggests a competitive reaction mechanism between Cl_2 and CH_4 to remove the group-III etch product. The GaN and InN etch rates are greater with the addition of CH_4 to the plasma chemistry. This may be attributed to the formation of the group-III methyl etch product or an etch mechanism enhanced by the presence of CH_4. Surface morphologies have been evaluated and quantified using AFM for GaN and InN. Very smooth pattern transfer has been obtained for a wide range of plasma conditions for GaN, however, the surface morphology of the etched InN surface is more sensitive to rf-power, microwave power, and process pressure. Using Auger spectroscopy we have observed a general tendency for the Ga:N ratio to increase with increasing rf-power or microwave power and to be independent of temperature.

ACKNOWLEDGMENTS

The authors would like to thank P. L. Glarborg and L. Griego for their technical support. This work was performed at Sandia National Laboratories supported by the U.S. Department of Energy under contract # DE-AC04-94AL85000.

DISCLAIMER

REFERENCES

1. S. Nakamura, T. Mukai, M. Seno, and N. Iwasu, Jpn. J. Appl. Phys. **31**, L139 (1992).
2. J. S. Foresi and T. D. Moustakas, Appl. Phys. Lett. **62**, 2859 (1993).
3. R. F. Davis. Proc. IEEE **79**, 702 (1991).
4. S. Nakamura, T. Mukai, and M. Senoh, Appl. Phys. Lett., **64**, 1687 (9194).
5. S. J. Pearton, C. R. Abernathy, P. Wisk, W. S. Hobson, and F. Ren, Appl. Phys. Lett. **63**, 1143 (1993).
6. S. C. Binari, L. B. Rowland, W. Kruppa, G. Kelner, K. Doverspike, and D. K. Gaskill, Electron. Lett. **30**, 1248 (1994).
7. S. Strite and H. Morkoc, J. Vac. Sci. Technol. B **10**, 1237 (1992).
8. M. A. Kahn, J. N. Kuzina, J. M. Van Hove, D. T. Olson, S. Krishnankutty, and R. M. Kolbas, Appl. Phys. Lett. **58**, 526 (1991).
9. T. L. Tansley and R. J. Egan, Phys. Rev. B **45**, 10942 (1993).
10. M. A. Khan, A. Bhattarai, J. N. Kuznia, and D. T. Olson, Appl. Phys. Lett. **63**, 1214 (1993).
11. T. Matsuoka, T. Sasaki, and A. Katsui, Optoelectronic Devices and Technologies, **5**, 53 (1990).
12. H. Amano, M. Kito, K. Hiramatsu, and I. Akasuki, Jpn. J. Appl. Phys. **28**, L2112 (1989).
13. S. Nakamura, M. Senoh, and T. Mukai, Jpn. J. Appl. Phys. **30**, L1708 (1991).
14. I. Akasaki, H. Amano, M. Kito, and K. Kiramatsu, Lumin. **48/49**, 666 (1991).
15. S. Nakamura, M. Senoh, and T. Mukai, Appl. Phys. Lett. **62**, 2390 (1993).
16. S. C. Binari, L. B. Rowland, W. Kruppa, G. Kelner, K. Doverspike, and D. K. Gaskill, Electron. Lett. **30**, 1248 (1994).
17. A. M. Khan, J. N. Kuznia, A. R. Bhattarai, and D. T. Olson, Appl. Phys. Lett. **62**, 1248 (1993).
18. C. Constantine, D. Johnson, S. J. Pearton, U. K. Chakrabarti, A. B. Emerson, W. S. Hobson, and A. P. Kinsella, J. Vac. Sci. Technol. **B 8**, 596 (1990).
19. S. J. Pearton, U. K. Chakrabarti, A. P. Kinsella, D. Johnson, and C. Constantine, Appl. Phys. Lett. **56**, 1424 (1990).
20. A. J. Murrell, R. C. Grimwood, P. O'Sullivan, M. Gilbert, K. Vanner, F. Ruddell, I. Davies, K. Hilton, S. Bland, and D. Spear, Technical Digest, Proc. 1992 GaAs IC Symposium, 173.
21. R. Cheung, Y. H. Lee, K. Y. Lee, T. P. Smith, III, D. P. Kern, S. P. Beaumont, and C. D. W. Wilkinson, J. Vac. Sci. Technol. **B 7**, 1462 (1989).
22. K. K. Ko and S. W. Pang, J. Electrochem. Soc. **141**, 250 (1994).
23. S. J. Pearton, F. Ren, T. R. Fullowan, J. R. Lothian, A. Katz, R. F. Kopf and C. R. Abernathy, Plasma Sources Sci. Technol. **1**, 18 (1992).
24. S. J. Pearton, C. R. Abernathy, and F. Ren, Appl. Phys. Lett. **64**, 2294 (1994).
25. C. Constantine, C. Baratt, S. J. Pearton, F. Ren, and J. R. Lothian, Appl. Phys. Lett. **61**, 2899 (1992).
26. C. R. Abernathy, J. Vac. Sci. Technol. A **11**, 869 (1993).
27. T. L. Chu, J. Electrochem. Soc. **119**, 1200 (1971).
28. J. I. Pankove, J. Electrochem, Soc. **119**, 1118 (1972).
29. T Y. Sheng, Z. Q. Yu, and G. J. Collins, Appl. Phys. Lett. **52**, 576 (1988).
30. T. Pauleau, J. Electrochem. Soc. **129**, 1045 (1982).

31. K. M. Taylor, and C. Lenie, J. Electrochem. Soc. **107**, 308 (1960).
32. *G. Long and L. M.* Fuster, J. Am. Ceram. Soc. **42**, 53 (1959).
33. N. J. Barrett, J. D. Grange, B. J. Sealy, and K. G. Stephens, J. Appl. Phys. **57**, 5470 (1985).
34. C. R. Aita and C. J. Gawlak, J. Vac. Sci. Technol. **A1**, 403 (1983).
35. G. R. Kline and K. M. Lakin, Appl. Phys. Lett. **43**, 750 (1983).
36. J. R. Mileham, S. J. Pearton, C. R. Abernathy, J. D. MacKenzie, R. J. Shul, and S. P. Kilcoyne, Appl. Phys. Lett., submitted.
37. I. Adesida, A. Mahajan, E. Andideh, M. Asif Khan, D. T. Olsen, and J. N. Kuzina, Appl. Phys. Lett. **63**, 2777.
38. M. E. Lin, Z. F. Zan, Z. Ma. L. H. Allen, and H. Morkoc, Appl. Phys. Lett. **64**, 887 (1994).
39. A. T. Ping, I. Adesida, M. Asif Khan, and J. N. Kuzina, Electron. Lett. **30**, 1895 (1994).
40. S. J. Pearton, C. R. Abernathy, F. Ren, J. R. Lothian, P. W. Wisk, A. Katz, and C. Constantine, Semicond. Sci. Technol. **8**, 310 (1993).
41. S. J. Pearton, C. R. Abernathy, and F. Ren, Appl. Phys. Lett. **64**, 2294 (1994).
42. S. J. Pearton, C. R. Abernathy, and F. Ren, Appl. Phys. Lett. **64**, 3643 (1994).
43. G. F. McLane, L. Casas, S. J. Pearton, and C. R. Abernathy, (to be published).
44. I. Adesida, A. T. Ping, C. Youtsey, T. Dow, M. Asif Khan, D. T. Olson, and J. N. Kuzina, Appl. Phys. Lett. **65**, 889 (1994).
45. R. J. Shul, S. P Kilcoyne, M. Hagerott Crawford, J. E. Parmeter, C. B. Vartuli, C. R. Abernathy, and S. J. Pearton, Appl. Phys. Lett. **66**, 1761 (1995).
46. R. J. Shul, A. J. Howard, S. J. Pearton, C. R. Abernathy, C. B. Vartuli, P. A. Barnes, and M. J. Bozack, J. Vac. Sci. Technol. B, submitted.
47. C. Constantine, private communication.
48. C. Constantine, C. Barratt, S. J. Pearton, F. Ren, and J. R. Lothian, Electron. Lett. **28**, 1749 (1992).